



Dual-kind Q-switching of erbium fiber laser

Yuri O. Barmenkov, Alexander V. Kir'yanov, Jose L. Cruz, and Miguel V. Andres

Citation: *Applied Physics Letters* **104**, 091124 (2014); doi: 10.1063/1.4867888

View online: <http://dx.doi.org/10.1063/1.4867888>

View Table of Contents: <http://scitation.aip.org/content/aip/journal/apl/104/9?ver=pdfcov>

Published by the [AIP Publishing](#)

Articles you may be interested in

[Self-Q-switching behavior of erbium-doped tellurite microstructured fiber lasers](#)

J. Appl. Phys. **115**, 223103 (2014); 10.1063/1.4883242

[Linearly polarized, Q-switched Er-doped fiber laser based on reduced graphene oxide saturable absorber](#)

Appl. Phys. Lett. **101**, 241106 (2012); 10.1063/1.4770373

[Self-balanced Q- and gain-switched erbium all-fiber laser](#)

AIP Advances **1**, 032155 (2011); 10.1063/1.3639132


[Phase locking of nanosecond pulses in a passively Q-switched two-element fiber laser array](#)

Appl. Phys. Lett. **90**, 151110 (2007); 10.1063/1.2721390

[Passive Q-switching of fiber lasers using a broadband liquefying gallium mirror](#)


Appl. Phys. Lett. **74**, 3619 (1999); 10.1063/1.123200

Agilent's Electronic Measurement Group is becoming **Keysight Technologies**.



Engineering Education & Research Resources DVD 2014

Agilent is the key to your test and measurement needs **Order yours**



Dual-kind Q-switching of erbium fiber laser

Yuri O. Barmenkov,^{1,a)} Alexander V. Kir'yanov,¹ Jose L. Cruz,² and Miguel V. Andres²

¹*Centro de Investigaciones en Optica, Loma del Bosque 115, Col. Lomas del Campestre, 37150 Leon, Guanajuato, Mexico*

²*Department of Applied Physics and Electromagnetism, University of Valencia, Dr. Moliner 50, Burjassot 46100, Spain*

(Received 19 November 2013; accepted 24 February 2014; published online 6 March 2014)

Two different regimes of Q-switching in the same implementation of an actively Q-switched erbium-doped fiber laser are demonstrated. Depending on the active fiber length and repetition rate of an intracavity Q-cell (acousto-optic modulator), the laser operates either in the regime of common, rather long and low-power, pulses composed of several sub-pulses or in the one of very short and powerful stimulated Brillouin scattering-induced pulses. The basic physical reason of the laser system to oscillate in one of these two regimes is the existence or absence of CW narrow-line “bad-cavity” lasing in the intervals when the Q-cell is blocked. © 2014 AIP Publishing LLC. [<http://dx.doi.org/10.1063/1.4867888>]

Actively Q-switched (QS) fiber lasers (FLs) producing high-power short pulses attract significant interest for many years. Active QS in FLs is usually implemented by means of acousto-optic modulators (AOMs), basically because of such advantages of this type of modulators as high modulation contrast (~ 50 dB), fast temporal response (10–100 ns), and the broad range of repetition rates f_{AOM} (DC—1 MHz). The featuring properties of QS FLs are a long interaction length of pump light with the active fiber core, permitting a high charge and correspondingly high gain in the fiber, together with single transversal mode operation.

QS FLs implemented in Fabry-Perot configuration using AOMs are capable to produce pulses (further QS pulses) ranged from a few to hundreds nanoseconds in duration.¹ Such pulses normally consist of several sub-pulses separated by an interval equal to round-trip time of a photon traveling through the cavity; let us further refer this regime to as “common” QS (CQS).^{2,3} The multi-peak shape of CQS pulses as well as their energetic parameters can be precisely reproduced applying the model of two contra-propagating laser waves.^{3,4} This model was shown to be helpful in predicting and experimental fulfilling the measures for shaping CQS pulses⁵ and, in particular, forming lone short pulses instead of multi-peak ones,⁶ which is invaluable for technological applications.

In the meantime, it is known that in some erbium and ytterbium QS FLs, stimulated Brillouin scattering (SBS) leads to SBS-induced stochastic self-QS pulsing,^{7,8} featured by dramatic increasing of pulse power as compared to CQS and by perceptible pulse amplitude and timing jitters.⁹ As shown by Kir'yanov *et al.*,¹⁰ both jitters at SBS-QS notably depend upon intra-cavity loss: at the higher loss, the jitter is smaller (which holds however if loss is not so high to prevent lasing).

In this Letter, we report a study of the two pulsed regimes, CQS and SBS-QS, obtained using the same experimental setup, an actively QS erbium-doped FL (EDFL) with an AOM Q-cell, built in Fabry-Perot geometry. The only

varied quantities therein are the active fiber length and AOM repetition rate; we show that type of QS established in the laser depends on both the parameters. On one hand, if active fiber is short the laser operates in CQS regime at any repetition rate; QS pulses in this case have multi-peak structure and negligible jitter.^{11,12} Worth noticing, such QS lasing is nothing than amplified spontaneous emission (ASE) propagating a finite number of passes between the laser couplers (fiber Bragg gratings, FBGs) after switching AOM on, whilst their multi-peak structure is ASE “bursts” at the laser output after each round-trip. On the other hand, if active fiber is long enough, the laser operates in CQS regime at high repetition rates only, whereas at low ones it enters SBS-QS pulsing; pulse jittering in the latter case is severe. We demonstrate that a necessary condition for SBS-QS to arise is the presence of CW narrow-line lasing in the intervals when the cavity is “blocked” (i.e., at closed AOM) and that CW lasing is developing spuriously due to the high gain in a strongly charged active fiber and weak feedback inside “bad cavity,” established by the output FBG coupler and internal back-reflection inside AOM (~ -40 dB). Furthermore, when the “main” cavity of QS EDFL, composed of two FBGs, becomes “unblocked” (i.e., when AOM gets opened), this spurious intra-cavity CW lasing plays the role of a seeding signal at establishing SBS-QS operation.

The scheme of our QS EDFL is shown in Figure 1. A fiber-coupled semiconductor laser (*JDSU*, 976 nm) was used for in-core pumping of a standard low-doped EDF (*Thorlabs*, M5-980-125) through a 980/1550-nm wavelength division multiplexer (WDM). The laser cavity consisted of a length L_{EDF} of EDF, varied between 3 and 9 m, a fiber-coupled AOM (*Gooch & Housego*) with operation wavelength 1550 nm, acoustical frequency 111 MHz, and rise time of ~ 30 ns, and two FBGs (1 and 2) with reflection coefficients/3-dB bandwidths at Bragg (laser) wavelength (~ 1549.4 nm) being $\sim 30\%/160$ pm and $\sim 100\%/265$ pm, respectively. When AC voltage at 111 MHz was applied to AOM, a collimated input beam was switched between the zero (“OFF-state”) and the first (“ON-state”) diffraction orders, the latter being AOM's output. A long-period grating (LPG) placed in between FBG1

^{a)}Author to whom correspondence should be addressed. Electronic mail: yuri@cio.mx

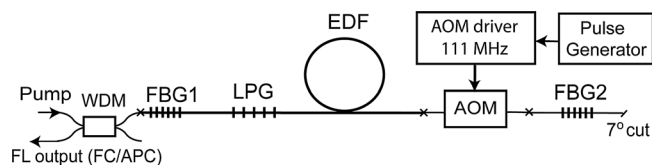


FIG. 1. Experimental setup: crosses indicate fiber splices. To diminish the overall cavity loss, FBG1 and LPG were written directly in the EDF after preliminary hydrogenation. AOM is driven by an AC voltage source with RF frequency of 111 MHz, controlled by a fast pulse generator.

and EDF, tunable around ~ 1530 nm (an Er^{3+} SE peak), was added in the laser scheme as in-line stop-band filter (with rejection peak of 23 dB and 3-dB bandwidth of ~ 6 nm) for neutralizing EDF gain at 1530 nm and, thereafter, avoiding lasing at this wavelength, extremely undesirable as competing with 1549.4-nm lasing, given by selectivity of FBGs. The laser signal was measured by means of an optical spectrum analyzer (OSA, 50-pm resolution) and a photodetector (1.2-GHz RF bandwidth), connected to a 2.5 GHz-oscilloscope. Pump power (500 mW) and AOM gate ($2 \mu\text{s}$) in all experiments were fixed.

Figure 2 shows the two optical spectra obtained for $L_{\text{EDF}} = 8.8$ m and blocked laser cavity (AOM is in OFF state; f_{AOM} is zero). When LPG is detuned from the optimal position (Figure 2(a)), CW lasing at ~ 1533 nm dominates, whereas when it is tuned to ~ 1533 nm (Figure 2(b)) CW lasing at ~ 1549.4 nm (the wavelength selected by FBG1) is observed.

It is known that CW EDFLs with FBG cavity couplers usually have a narrow spectrum line of about tenths MHz,^{13,14} thus, a coherence length of laser radiation is comparable with a FL's cavity length (~ 10.4 m as maximum in our case). Moreover, in some works, spectral width of lasing in CW EDFL was reported to be of the order of tenths kHz.¹⁵ This feature is an important chain in the discussion of dual nature of QS regime in our laser, see below.

When L_{EDF} is large, the laser demonstrates rich dynamics that strongly depends on AOM's repetition rate f_{AOM} . Figure 3 exemplifies the two qualitatively different QS regimes obtained at $L_{\text{EDF}} = 7.6$ m. High f_{AOM} -values lead to establishing in the laser of CQS regime where pulses consist of several sub-pulses (see Figure 3(a)). Such pulses are delayed with respect to the moment when AOM is switched ON (zero time)

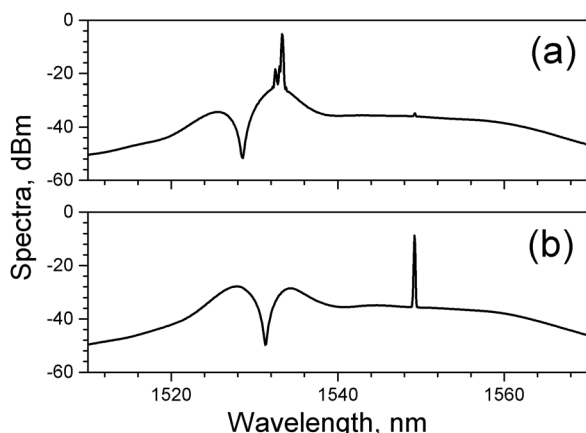


FIG. 2. FL output spectra when AOM is blocked. (a) LPG is detuned from and (b) tuned to the SE spectral maximum for eliminating spurious lasing at 1533 nm. EDF length is 8.8 m.

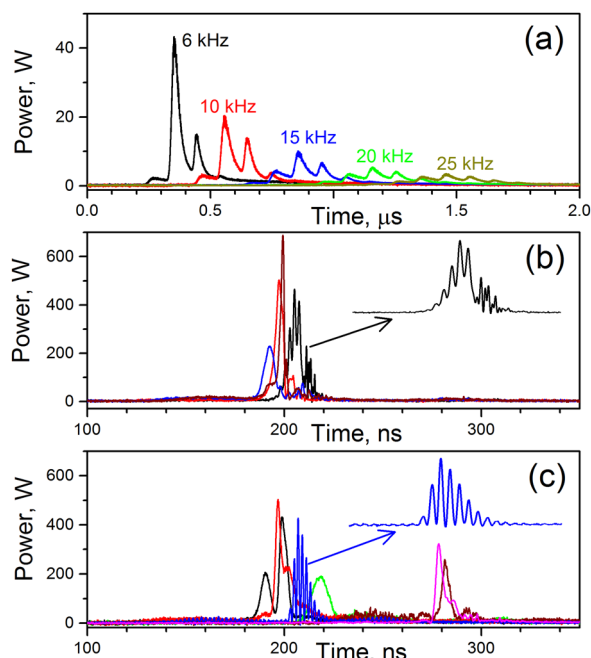


FIG. 3. Snapshots of QS pulses observed at (a) high AOM repetition rates (≥ 6 kHz) and at low repetition rates (b) 1 kHz and (c) 4 kHz. Each pulse corresponds to a separate experimental realization.

by an interval equal to a few photon round-trips in the cavity. Furthermore, this delay grows with f_{AOM} ; for instance, at $L_{\text{EDF}} = 7.6$ m, the first detectable sub-pulse arises after ~ 2.5 round-trips (~ 250 ns) at $f_{\text{AOM}} = 6$ kHz, ~ 4.5 round-trips (~ 450 ns) at $f_{\text{AOM}} = 10$ kHz, and so on. Accordingly, pulse amplitude decreases whilst number of sub-pulses increases. The maximal power/energy of QS pulses in this regime is ~ 40 W/ $2.5 \mu\text{J}$, respectively, and the minimal duration at a 3-dB level of the most powerful sub-pulse is ~ 40 ns (the entire pulse width is ~ 300 ns). Note that similar behavior was observed for other L_{EDF} . Emphasize that CQS pulsing is simply the ASE wave reflected several times from the selective FBGs, which looks in the time domain as multi-peak structure or sub-pulses (see Figure 4 and the discussion below). This process, being in fact not lasing but a regime of multi-pass ASE amplifying, continues until the active EDF gets discharged down to a certain inversion level that depends upon the values of excited state absorption at the operation wavelength¹⁶ and cavity loss.¹¹

In contrast, at f_{AOM} less than 6 kHz (see Figures 3(b) and 3(c)), the laser dynamics is completely different as compared to the previous case. Namely, pulses at such f_{AOM} arise earlier (~ 180 – 280 ns after the moment of AOM's switching ON) and their amplitudes are by ~ 10 – 15 dB bigger than at CQS. The other difference is that pulses generated at low f_{AOM} are much narrower (~ 2.5 – 10 ns at a 3-dB level), more energetic (pulse energy is $\sim 4.5 \mu\text{J}$), and their shapes are apparently not common. As shown below by means of a spectral analysis, this regime is a kind of SBS-QS pulsing. Notice that no SBS-QS pulses exist within the intervals between the adjacent AOM's gates, in contrast to SBS-QS pulses in ytterbium-doped FLs.^{9,10}

One more detail of SBS-QS is that pulses in this regime suffer strong amplitude and timing jitters. Apparently, jittering itself is an indication of the stochastic nature of the SBS

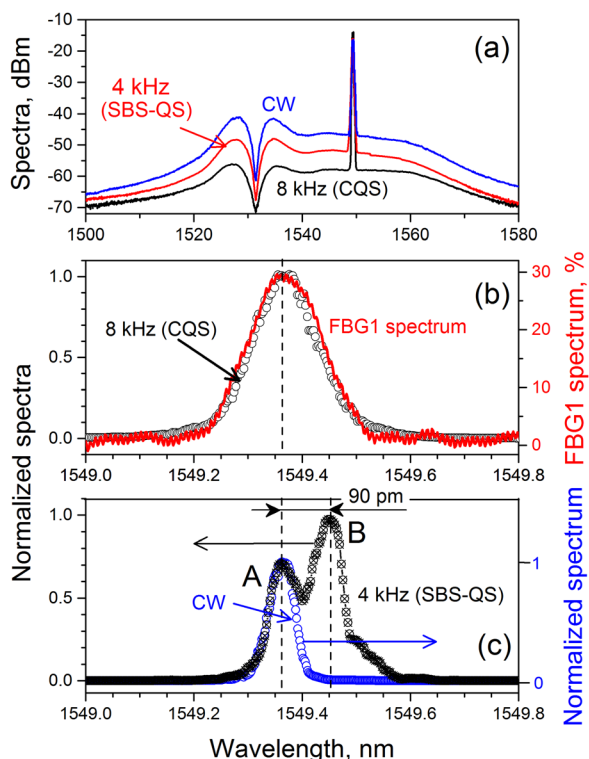


FIG. 4. (a) FL optical spectra recorded at EDFL operation in CW regime when its cavity is always blocked (upper curve), in SBS-QS regime at $f_{\text{AOM}}=4$ kHz (middle curve), and in CQS regime at $f_{\text{AOM}}=8$ kHz (lower curve). (b) Normalized FL spectra measured at $f_{\text{AOM}}=8$ kHz (black open circles, left scale) and FBG1 spectrum (red solid curve, right scale). (c) Normalized FL spectra measured at $f_{\text{AOM}}=4$ kHz (black crossed circles) and at continuously blocked AOM (CW lasing, blue open circles). Spectrum of CW lasing is normalized to demonstrate that its maximum matches the maximum of peak A.

process involved. Furthermore, as seen from comparison of Figures 3(b) and 3(c), timing jitter grows with increasing f_{AOM} : at $f_{\text{AOM}}=1$ kHz (far from 6 kHz where CQS arises; refer to Figure 3(b) as an example), it is limited by ~ 20 ns, whereas at $f_{\text{AOM}}=4$ kHz (closer to the 6-kHz limit) SBS-QS pulses get spread into two groups, differing by approximately one round-trip time in the arising moment (~ 200 ns and ~ 290 ns), which in turn enlarges the jitter by several times.

The effect of spreading SBS-QS pulses into two groups at high repetition rates (Figure 3(c)) may be explained in the following way. At increasing f_{AOM} , the EDF's charge (established just before AOM's switching ON) decreases, which reduces both the EDF's gain and power of CW lasing in the "bad cavity." Hence, at higher f_{AOM} , the CW laser wave propagating inside the cavity needs more time for amplifying to accomplish the SBS-threshold's condition. As the adjacent leading edges of the narrow-line CW laser wave responsible for creating SBS-gratings differ in time by one round-trip, the resultant SBS-QS pulses become delayed accordingly, i.e., by approximately one round-trip time. Due to the stochastic nature of Brillouin scattering, this results in delaying of SBS-QS pulses by intervals equal to either two (~ 200 ns) or three (~ 290 ns) round-trip times and, correspondingly, in enlarging of timing jitter. In contrast, at lower f_{AOM} the EDF's charge is sufficient for the narrow-line CW wave to reach SBS threshold at the moments enabling SBS-QS pulses form only the first group.

As seen from the insets to Figures 3(b) and 3(c), some of SBS-QS pulses are smooth and narrow while others are modulated up to $\sim 100\%$. A reason of such modulation can be that pulses are born by a seed CW signal, being a superposition of two simultaneously oscillating longitudinal modes (a FFT analysis has shown that the beating frequencies are 418 and 486 MHz, corresponding to 43 and 50 intermodal intervals, respectively). We have checked the presence of a beating frequency in the output signal at CW lasing (when AOM was continuously in OFF state) and found that either a single mode (no beating) or a couple of modes (with ~ 8 –50 intermodal intervals) randomly oscillates in the "bad cavity." Supposedly, these two types of intra-cavity seed radiation lead to SBS-QS pulsing in the forms of smooth or strongly modulated pulses.

Finally, note that SBS-QS operation is not observed when EDF length is less than a certain value ($L_{\text{EDF}} \sim 5.3$ m).

Let us consider the spectral features of the EDFL when $L_{\text{EDF}}=7.6$ m, see Figure 4. We shall show that pulsing of the first type (CQS) starts developed from ASE, whereas the second one (SBS-QS) is "ignited" by CW "bad-cavity" lasing, occurring when AOM is OFF; this CW radiation is seeded into the main cavity formed by both FBGs (when AOM gets opened) and effectively boosts the SBS process.

For better understanding the dual kind of QS pulsing, we zoom the spectra plotted in Figure 4(a) for shading light on the laser-line proximity's properties in each of the cases discussed above: $f_{\text{AOM}}=0$, 4, and 8 kHz, see Figures 4(b) and 4(c).

Comparing the optical spectra at CQS ($f_{\text{AOM}}=8$ kHz) and SBS-QS ($f_{\text{AOM}}=4$ kHz), one sees that in the former case the spectrum (Figure 4(b)) virtually repeats the reflection spectrum of FBG1 (the one of FBG2 is broader), whereas in the latter (Figure 4(c), see the two-peak spectrum)—it consists of two spectral lines A and B, spaced by ~ 90 pm (~ 11 GHz, the Brillouin shift in the frequency domain). Both lines A and B are narrower (~ 55 –60 pm, measured by the OSA with a 50-pm resolution) than the CQS (ASE) spectrum (~ 160 pm). Supposedly, the line A, centered at the FBG1's peak, corresponds to CW lasing arisen when AOM is in OFF state (i.e., between the adjacent AOM gates) whereas the line B—to SBS-QS pulsing. To provide more argumentation in favor of the hypothesis, we plot in Figure 4(c) the spectrum of CW lasing obtained when the main cavity is always blocked (i.e., AOM is continuously in OFF state). It is seen that the line A (at SBS-QS, $f_{\text{AOM}}=4$ kHz) vastly reproduces the CW lasing spectrum. This supports our idea that the narrow line A is the signature of CW lasing and that it initiates the SBS-process. Accordingly, the narrow line B, shifted by ~ 90 pm to the Stokes side, is the signature of SBS-induced pulsing.

Analyses similar to the one presented in Figure 4, made for other EDF lengths, have shown that virtually all spectral laws revealed above apply to any cavity length at which CQS and SBS-QS regimes coexist. Overview of the whole pattern of the dual-kind QS, parameterized in terms of f_{AOM} vs. L_{EDF} , is depicted by Figure 5(a).

It is seen that the f_{AOM} -range in which SBS-QS develops (the area below the solid line in Figure 5(a)) is narrowed with decreasing EDF length. In other words, the minimal

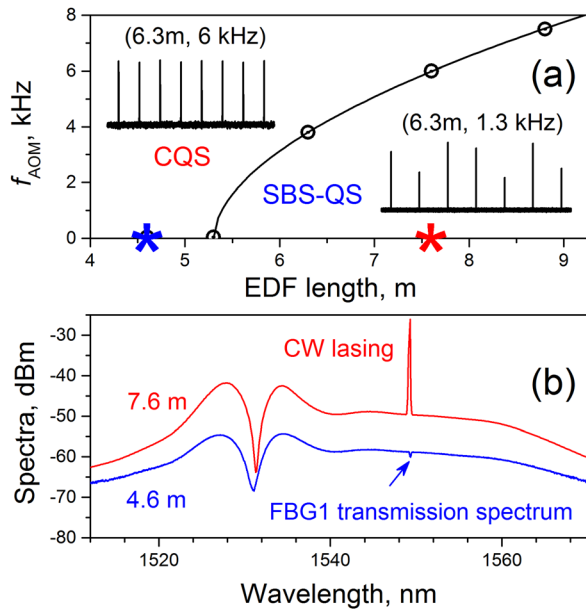


FIG. 5. (a) Basins of CQS and SBS-QS operations in terms of f_{AOM} vs. L_{EDF} . Symbols depict the experimental data on the border between the CQS and SBS-QS basins and the solid line is a fit. (b) Typical spectra observed when the EDFL cavity is blocked ($L_{\text{EDF}} = 4.6\text{ m}$ and 7.6 m).

f_{AOM} -value at which CQS pulses develop (the area above the solid line in Figure 5(a)) shifts down. If EDF length is less than or equal to a certain value ($L_{\text{EDF}} = 5.3\text{ m}$ in our arrangement), the laser operates solely in CQS regime, at any f_{AOM} . To emphasize the difference in pulse jittering in these two cases, two pulse trains are snapshotted in Figure 5(a): it is seen that jitter at SBS-QS is very strong but it does not exist at CQS at all.

The experimental points designating the boundary between the areas, or basins, of CQS and SBS-QS regimes are fitted well by a square root function (see the black line in the figure). Note that quite similar long-term statistics of pulsing with (SBS-QS) and without (CQS) jitter is observed in the whole of the subareas below and above the boundary line.

We also provide (see Figure 5(b)) the typical optical spectra measured at the EDFL cavity blocked for other EDF lengths, $L_{\text{EDF}} = 4.6$ and 7.6 m (these two realizations are marked in Figure 5(a) by the blue and red asterisks, respectively). It is seen (compare Figures 5(a) and 5(b)) that when EDF is longer than 5.3 m , CW lasing always exists (see the red spectrum in Fig. 5(b)), whereas when EDF is shorter than 5.3 m there is no lasing (see the blue spectrum in Figure 5(b)). Noteworthy, in the second case, there appears the FBG1 transmission peak instead of CW lasing. This detail supports the hypothesis that the “bad-cavity” spurious CW lasing is the key mechanism for SBS-QS pulsing.

In summary, we have demonstrated that two different scenarios of QS pulsing happen in an actively QS-EDFL with AOM and that type of pulsing severely depends on the EDF length and AOM’s repetition rate. That is, if EDF is short or/and repetition rate is high, the laser operates in CQS regime where pulses have multi-peak structure with sub-pulses spaced by the cavity round-trip time. Otherwise, if EDF is long and AOM’s repetition rate is low, the laser enters SBS-QS regime; in this case, pulse energy is about two times bigger than at CQS. We have also showed that the cause for one or another QS regime to develop in the QS-EDFL is the presence or absence of narrow-line CW lasing in the intervals when AOM is in OFF state, which is in turn defined by the values of repetition rate and EDF length. That is, when AOM is open, on one hand, the narrow-line “bad-cavity” CW radiation plays, if presents, the role of seed for SBS-QS pulsing, whereas, on the other hand, if it does not, the ASE wave forms multi-peak CQS pulses during a few round-trips of light in the main (unblocked) cavity, within an AOM’s gate.

Authors acknowledge support from the CONACyT, Mexico (Project No. 167945) and from the Ministerio de Economía y Competitividad and the Generalitat of Valencia, Spain (Project Nos. TEC2008-05490 and PROMETEO-2009-077, respectively).

- ¹D. J. Richardson, J. Nilsson, and W. A. Clarkson, *J. Opt. Soc. Am. B* **27**, B63 (2010).
- ²E.-L. Lim, S.-U. Alam, and D. J. Richardson, *IEEE Photonics Technol. Lett.* **23**, 1763 (2011).
- ³S. A. Kolpakov, Y. O. Barmenkov, A. D. Guzman-Chavez, A. V. Kir’yanov, J. L. Cruz, A. Diez, and M. V. Andres, *IEEE J. Quantum Electron.* **47**, 928 (2011).
- ⁴Y. Wang and C.-Q. Xu, *Opt. Lett.* **29**, 1060 (2004).
- ⁵L. Escalante-Zarate, Y. O. Barmenkov, J. L. Cruz, and M. V. Andres, *IEEE Photonics Technol. Lett.* **24**, 312 (2012).
- ⁶L. Escalante-Zarate, Y. O. Barmenkov, S. A. Kolpakov, J. L. Cruz, and M. V. Andres, *Opt. Express* **20**, 4397 (2012).
- ⁷A. A. Fotiadi and P. Megret, *Opt. Lett.* **31**, 1621 (2006).
- ⁸L. Pan, I. Utkin, R. Lan, Y. Godwal, and R. Fedosejevs, *Opt. Lett.* **35**, 895 (2010).
- ⁹Y. O. Barmenkov, A. V. Kir’yanov, and M. V. Andres, *IEEE J. Quantum Electron.* **48**, 1484 (2012).
- ¹⁰A. V. Kir’yanov, Y. O. Barmenkov, and M. V. Andres, *Laser Phys. Lett.* **10**, 055112 (2013).
- ¹¹Y. O. Barmenkov, S. A. Kolpakov, A. V. Kir’yanov, L. Escalante-Zarate, J. Luis Cruz, and M. V. Andres, *IEEE Photonics Technol. Lett.* **25**, 977 (2013).
- ¹²S. A. Kolpakov, Y. O. Barmenkov, A. Kir’yanov, L. Escalante-Zarate, J. L. Cruz, and M. V. Andres, *IEEE Photonics Technol. Lett.* **25**, 480 (2013).
- ¹³S. V. Chernikov, J. R. Taylor, and R. Kashyap, *Opt. Lett.* **18**, 2023 (1993).
- ¹⁴A. D. Guzman-Chavez, Y. O. Barmenkov, A. V. Kir’yanov, and F. Mendoza-Santoyo, *Opt. Commun.* **282**, 3775 (2009).
- ¹⁵K. N. Choi and H. F. Taylor, *IEEE Photonics Technol. Lett.* **15**, 386 (2003).
- ¹⁶A. D. Guzman-Chavez, Y. O. Barmenkov, and A. V. Kir’yanov, *Appl. Phys. Lett.* **92**, 191111 (2008).